PHYSICAL REVIEW B VOLUME 5, NUMBER 4 15 FEBRUARY 1972

High-Field Isothermal Currents and Thermally Stimulated Currents in Insulators Having Discrete Trapping Levels

J. G. Simmons and G. W. Taylor
Electrical Engineering Department, University of Toronto, Toronto, Canada
(Received 21 June 1971)

The theory is developed for the isothermal and thermally stimulated currents (TSC) which flow in optically excited insulators that are subjected to high fields. The conditions for high-field and low-field TSC are defined. The high-field process is theoretically attractive since only first-order kinetics are required to describe the dynamics involved. In addition, the boundary conditions for TSC have been clearly defined for the first time. The isothermal current for a discrete trap is shown to be an exponential decay in time. The transcendental equations that result for the TSC are analyzed in considerable detail, with the result that corresponding approximate analytical expressions have been deduced which will considerably expedite the analyses of experimental data. A detailed discussion is given of the application of the theory to experimental data.

I. INTRODUCTION

The study of thermally stimulated currents (TSC) in solids is potentially a powerful method of determining the defect nature of semiconductors and insulators. However, the complete description of TSC, for an arbitrary distribution of trapping levels and recombination centers, has produced differential equations that have proved intractable. As a result, workers in the past have resorted to various approximations and very simple insulator models. These assumptions and models have now become, more or less, the foundation of current theoretical studies. Thus the more recent treatments[1] of the subject differ only in detail rather than principle from earlier work.[2–6]

The assumptions regarding the physical model are severely restrictive because they are applicable only to the simplest of trapping conditions, which can seldom, if ever, be related to a real material. Saunders[3] has summarized and discussed these assumptions in detail. For even the simplest of models, it is extremely difficult to correlate theory and experiment with any degree of confidence, because of the intractability of the pertinent theoretical equations and the number and uncertainty of the physical parameters involved. Indeed, Kelly and Braunlich[2] have very recently noted that "simultaneous experiments on TSC (and thermally stimulated luminescence) do not yield sufficient information to determine the kinetical mechanism of the thermally stimulated recombination process without *a priori* knowledge of most of the trapping parameters."

The object of this paper is to treat the problem of thermally stimulated currents, in the presence of high fields, in insulators with blocking contacts. The theoretical advantages of the high-field TSC treatment over that of the conventional low-field, Ohmic-contact case is that retrapping can be certainly ignored; that is, first-order kinetics apply. The method is applicable to reverse-biased p-n junctions, metal-oxide-semiconductor interfaces, and to thin insulating and semiconducting films.

II. GENERAL KINETIC EQUATIONS

A. Initial Conditions

Consider an insulator containing an arbitrary distribution of discrete trapping levels throughout its band gap. When the solid is in thermal equilibrium, traps below the equilibrium Fermi energy E_{F0} are essentially full and those above it are essentially empty. Consider the case when the traps are excited by optical stimulation when the solid is at a constant low temperature T_0. We will assume that the illumination source intensity and wavelength are selected to produce a uniform absorption of light throughout the region of the solid to be investigated. In the past, the initial boundary condition (i.e., the excitation of the traps) has been assumed to be quite arbitrary. In actual fact the excitation of the traps is determined essentially by nonequilibrium steady-state statistics.[7] It can be shown that the initial occupancy of a trapping center under steady-state conditions such as those described above is given by

$$f_0(E_t) = \frac{\bar{n}_s + e_{p0}}{e_{n0} + \bar{n}_s + \bar{p}_s + e_{p0}}, \tag{1}$$

$$\bar{p}_s = v\sigma_p p_s, \tag{2}$$

$$\bar{n}_s = v\sigma_n n_s, \tag{3}$$

where n_s is the free-electron density in the steady state, v is the thermal velocity of an electron, σ_n is the capture cross section of the trap for electrons, p_s is free-hole density in the steady state, σ_p is the capture cross section of the trap for free

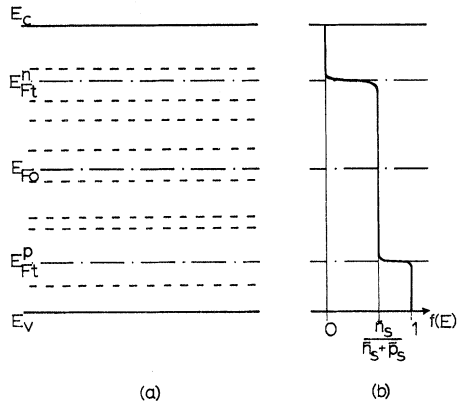

FIG. 1. (a) Energy diagram for an insulator with an arbitrary distribution of discrete trapping levels. (b) Occupancy function for the insulator after optical stimulation. Trapping levels are assumed to be members of a species (Ref. 7) $R(=\sigma_n/\sigma_p)$.

holes, $e_{n0}=v\sigma_n N_c\, e^{(E_t-E_c)/kT_0}$ is the emission coefficient for electrons out of the trap at temperature T_0, $e_{p0}=v\sigma_p N_v\, e^{(E_v-E_t)/kT_0}$ is the emission coefficient for holes out of the trap at temperature T_0, and E_t is the energy of the trap. Immediately after the light is turned off, there occurs a rapid decay of the free carriers in the conduction and valence bands. Since the free-carrier density is much smaller than the trap density, we assume that the capture of the free carriers by the traps does not significantly perturb the steady-state occupancy of the traps as given by (1). Thus, the initial conditions at the starting temperature T_0 can be adequately described by (1) (see Fig. 1). The importance of (1) in relation to the filling of the traps has been described in the previous paper,[7] to which the reader is referred for further details. However, it will be noted that the energy $E_t=E^n_{Ft}$ satisfying the relationship

$$e_n=\bar{n}_s+\bar{p}_s$$

or

$$v\sigma_n N_c\, e^{(E^n_{Ft}-E_c)/kT}=\bar{n}_s+\bar{p}_s \tag{4}$$

defines a quasi-Fermi level for trapped electrons. This is because trapping levels positioned above E^n_{Ft} are essentially empty and levels positioned below E^n_{Ft} are substantially occupied to a occupancy level given by

$$\bar{n}_s/(\bar{n}_s+\bar{p}_s). \tag{5}$$

In a similar manner, the energy E^p_{Ft} determined by

$$v\sigma_p N_v\, e^{(E_v-E^p_{Ft})/kT}=\bar{n}_s+\bar{p}_s \tag{6}$$

defines a quasi-Fermi level for trapped holes. Levels positioned below E^p_{Ft} are essentially devoid of holes and those above E^p_{Ft} are substantially occupied with holes to an occupancy level of

$$\bar{p}_s/(\bar{n}_s+\bar{p}_s)\ . \tag{7}$$

We assume that immediately after the collapse of the optically generated free carriers, a high field is applied to the insulator. This field is assumed to be sufficiently high so that the free carriers thermally excited out of the traps are pulled out of the insulator without being retrapped; that is, the lifetime of the carrier is greater than its transit time through the insulator. Furthermore, it is assumed that the applied field is sufficiently high so that any space-charge fields may be neglected; that is, the field in the insulator is essentially uniform. It is assumed that the contacts at the cathode and anode are blocking to electrons and holes, respectively, so that they are noninjecting. Thus the current flowing in the system is proportional to the rate of release of carriers from the traps.

B. General Current Equations

We will consider first a single trapping level and go on to generalize the results later. The rate of emission per unit volume of electrons to the conduction band is

$$\frac{dn_t}{dt}=e_n n_t\ , \tag{8}$$

where n_t is the number of electrons in the trapping level positioned at an energy E_t, and

$$e_n=v\sigma_n N_c\, e^{(E_t-E_c)/kT}$$

is the rate of emission of electrons from a level at energy E_t and temperature T. Hence the contribution to the current of electrons emitted from an incremental thickness dx of the insulator is

$$\delta I_n=qe_n n_t x\, dx/L, \tag{9}$$

where the distance x is measured from the cathode and L is the thickness of the insulator (see Fig. 2). Simarily, the contribution to the current by holes emitted to the valence band from dx is

$$\delta I_p=qe_p(N_t-n_t)\,(L-x)\,dx/L, \tag{10}$$

where N_t is the trap density of the trapping level positioned at energy E_t and

$$e_p=v\sigma_p N_t\ e^{(E_v-E_t)/kT}$$

is the rate of emission of holes from the trapping level at temperature T. Thus the total contribution to the current of carriers emitted from the incremental strip dx is, from (9) and (10),

$$\delta I=\delta I_n+\delta I_p=(q/L)[e_n n_t x+e_p(N_t-n_t)(L-x)]\,dx.$$

The total current flowing in the solid is therefore

given by

$$I=(q/L)\int_0^L [e_n n_t x+e_p (N_t-n_t)(L-x)]\,dx$$

$$=\tfrac{1}{2}q[e_n n_t+e_p(N_t-n_t)]L. \tag{11}$$

Although I is the current per unit cross-sectional area of the solid, it is not to be confused with current density, which is independent of the length of the solid.

The rate of change of the number of electrons in the trapping level is equal to the rate of emission of electrons to the conduction band minus the rate of emission of holes to the valence band. That is, we have

$$n_t'=-e_n n_t+e_p(N_t-n_t) \tag{12}$$

or

$$n_t'+(e_n+e_p)n_t=e_p N_t\,. \tag{13}$$

The solution to (13) is

$$n_t=e^{-h}\int_0^t e_p N_t e^h\,dt+C, \tag{14}$$

where $h=\int_0^t (e_n+e_p)\,dt$. In (14), C is an arbitrary constant determined by the boundary condition that at $t=0$ the number of electrons in the traps is $n_{t0}=N_t f_0$; thus from (1)

$$n_{t0}=N_t\left(\frac{\bar{n}_s+e_p}{e_n+\bar{n}_s+\bar{p}_s+e_p}\right). \tag{15}$$

From (14) and (15), we have

$$C=n_{t0}.$$

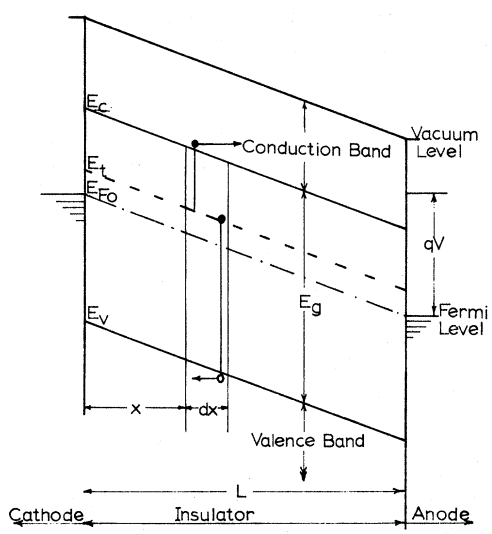

FIG. 2. Energy diagram for an insulator with an arbitrary distribution of discrete trapping levels subjected to a high field.

III. ISOTHERMAL CURRENT DECAY

A. Single Discrete Trap

At a constant temperature, for which e_n and e_p are constant in time, (14) is evaluated as

$$n_t=\left(n_{t0}-\frac{e_p N_t}{e_n+e_p}\right)e^{-(e_n+e_p)t}+\frac{e_p N_t}{e_n+e_p}. \tag{16}$$

From (16), we have

$$e_n n_t=e_n\left(n_{t0}-\frac{e_p N_t}{e_p+e_n}\right)e^{-(e_n+e_p)t}+\frac{e_p e_n N_t}{e_n+e_p}. \tag{17}$$

Using a similar procedure to that used in obtaining (17), one may derive the analogous equation for holes:

$$e_p(N_t-n_t)=e_p\left(p_{t0}-\frac{e_n N_t}{e_n+e_p}\right)e^{-(e_n+e_p)t}+\frac{e_n e_p N_t}{e_n+e_p}, \tag{18}$$

where

$$p_{t0}=N_t\left(\frac{p_s+e_n}{e_n+\bar{n}_s+\bar{p}_s+e_p}\right).$$

Thus, from (11), (17), and (18) the current flowing in the system is given by

$$I=\tfrac{1}{2}qL\left(e_n n_{t0}+e_p p_{t0}-\frac{2e_n e_p N_t}{e_n+e_p}\right)e^{-(e_n+e_p)t}+\frac{2e_n e_p N_t}{e_p+e_n}. \tag{19}$$

It is apparent from (19) that the current decays exponentially with time, with a time constant equal to $(e_n+e_p)^{-1}$. The second term on the right-hand side of (19) is simply the *constant* generation current flowing in the solid in the unexcited state.

B. Set of Discrete Traps

If a set of discrete levels exists in the insulator, the total current consists of the sum of the currents from each trapping level. When dealing with more than one trapping level it is convenient to reduce (19) to a simpler, more manageable form as follows. For levels such that $e_n \gg e_p$ (that is, levels above the intrinsic Fermi energy E_i), we have

$$I=\tfrac{1}{2}Lq\,e_n n_{t0}\,e^{-e_n t}\,, \tag{20}$$

and for levels such that $e_p \gg e_n$ (that is, levels below E_i),

$$I=\tfrac{1}{2}Lq\,e_n n_{t0}\,e^{-e_p t}\,. \tag{21}$$

Consider the case of an insulator containing two trapping levels, one positioned at an energy E_1 ($>E_i$) and of trap density N_{t1} per unit volume, and the other positioned at an energy E_2 ($<E_i$) and of trap density N_{t2} per unit volume. (This two-level system contains all the essential features of a more general system containing several discrete

levels.) Thus from (19), (18), and (7) we obtain

$$I=\frac{qL}{2(\bar{n}_s+\bar{p}_s)}\left(\bar{n}_s N_{t1}\, e_{n1}\, e^{-e_{n1}t}+\bar{p}_s N_{t2}\, e_{p2}\, e^{-e_{p2}t}\right),$$

where the second subscripts 1 and 2 on the various parameters refer, respectively, to the trap levels at E_1 and E_2. Normally, the time constants associated with the exponential terms e_{n1}^{-1} and e_{p2}^{-1} will differ significantly such that, say $e_{n1}^{-1} \gg e_{p2}^{-1}$. What this means is that initially ($t \lesssim e_{p2}^{-1}$) the current will decay with a time constant e_{n1}^{-1} and thereafter ($t \gtrsim e_{p2}^{-1}$) with a time constant e_{p2}^{-1}. Clearly, these remarks can be readily generalized to any system of discrete trapping levels.

IV. THERMALLY STIMULATED CURRENTS

A. Single Discrete Trapping Level

Thermally stimulated currents are observed in the excited system when the temperature is changed in a controlled manner after the field has been applied. Equation (8) is applicable to this case, but with the time related to the temperature through

$$T-T_0=\beta t, \tag{22}$$

where β is the *constant* heating rate in degrees per second. In this case both e_n and e_p are functions of time through the temperature T and the heating rate β. Hence, from (14) and (22), we obtain

$$n_t(T)=e^{-\lambda}\left(\beta^{-1}\int_{T_0}^{T} e_p N_t\, e^{\lambda}\, dT+n_{t0}\right),$$

where

$$\lambda=\beta^{-1}\int_{T_0}^{T}(e_n+e_p)\, dT. \tag{23}$$

Trapping levels positioned above E_i such that $e_n \gg e_p$ act essentially as electron emitting levels only; thus the terms containing e_p in (23) may be dropped yielding

$$n_t=n_{t0}\exp\left(-\beta^{-1}\int_{T_0}^{T} e_n\, dT\right). \tag{24}$$

From (11) and (24) the current flowing in the system associated with the emission of electrons from the traps is

$$I_n=\tfrac{1}{2}qL\, n_{t0}\, e_n\, e^{-\beta^{-1}\int_{T_0}^{T} e_n\, dT}. \tag{25}$$

On the other hand, levels positioned below E_i ($e_p \gg e_n$) act as essentially hole-emitting levels only. In this case it is relatively straightforward to show from (13) that the corresponding equation to (24) for holes is given by

$$p_t=p_{t0}\exp\left(-\beta^{-1}\int_{T_0}^{T} e_p\, dT\right). \tag{26}$$

From (11) and (26) the current flowing in the system associated with the emission of holes from these traps is

$$I_p=\tfrac{1}{2}qL\, p_{t0} e_p\exp\left(-\beta^{-1}\int_{T_0}^{T} e_p\, dT\right). \tag{27}$$

For the sake of conciseness we will confine our remarks to predominantly electron-emitting levels, but it will be apparent that a corresponding treatment can be applied equally as well to predominantly hole-emitting levels. The approximate solution to (24) is (see Appendix)

$$n_t \simeq n_{t0}\exp\left(-\frac{v\sigma_n N_c k T^2}{\beta(E_c-E_t+kt)}\, e^{(E_t-E_c)/kT}\right). \tag{28}$$

From (28) and (11) for $e_n \gg e_p$, the current flowing in the system

$$I=\tfrac{1}{2}qL\, n_{t0} e_n\exp\left(-\frac{v\sigma_n N_c k T^2}{\beta(E_c-E_t+kT)}\, e^{(E_t-E_c)/kT}\right). \tag{29}$$

The full curve in Fig. 3 illustrates a plot of I vs T using (29). This curve has a pronounced maximum and is representative of a typical high-field TSC curve. The dotted curve in Fig. 3 is a plot of I vs T using the exact intractable expression (25) and the same parameters as for the full curve. The correlation between the two curves is seen to be quite good.

The position of the peak in the thermally stimulated current is located by differentiating (24) and equating the result to zero. This yields[8]

$$\frac{\beta\Delta E}{kT_m^2}=v\sigma_n N_c\, e^{-\Delta E/kT_m}, \tag{30}$$

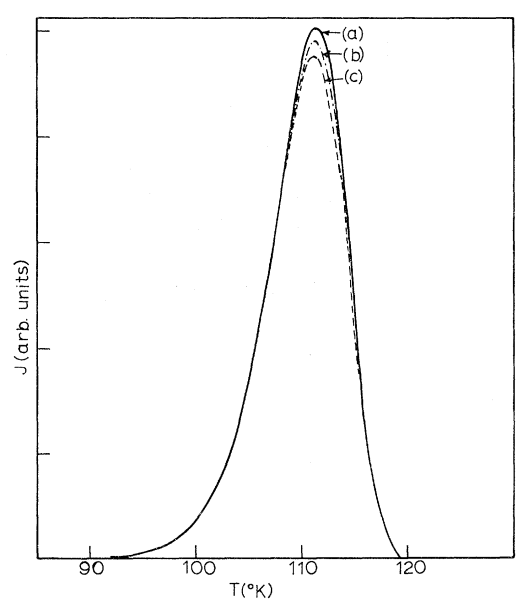

FIG. 3. J-T characteristic for a TSC curve illustrating (a) transcendental expression (25); (b) approximate analytical expression (29); and (c) approximate analytical curve obtained using (A6).

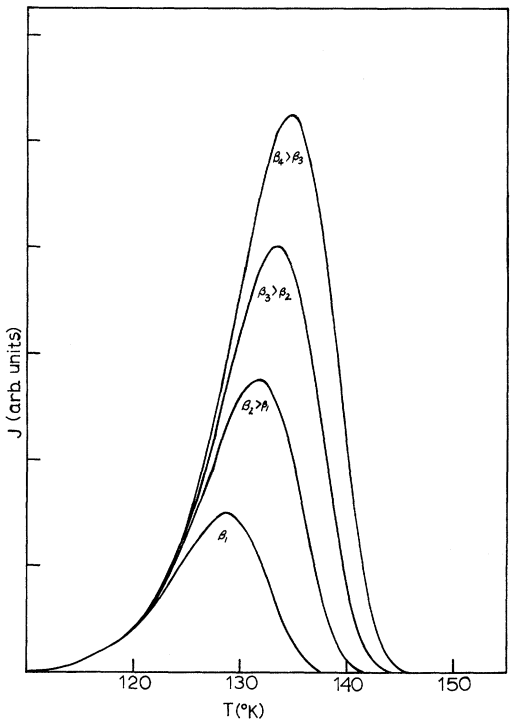

FIG. 4. J-T characteristic for a TSC curve for four different heating rates.

where T_m is the temperature at which the peak occurs, and $\Delta E = E_c - E_t$. From (29) and (30) the magnitude of the current at the maximum of the TSC curve is

$$I_m = \tfrac{1}{2} qL\, n_{t0} \frac{\beta \Delta E}{kT_m^2}\, e^{-\Delta E/(\Delta E + kT_m)} . \tag{31}$$

By performing an experiment at two different heating rates β_1 and β_2, (30) yields two relations from which ΔE and σ_n can be determined. From (31) it is seen that I_m increases linearly with β. The effect of β on the thermally stimulated curve is shown in Fig. 4 for a typical set of parameters. The variation of T_m with β and E_t will be discussed in Sec. V.

The area under the TSC curve A may be written [see Eq. (5)]

$$A = \int_{T_1}^{T_2} I\, dT, \tag{32}$$

but from (8) and (11) for, say, an electron-emitting trap,

$$A = \tfrac{1}{2} qL \int_{T_1}^{T_2} \frac{dn_t}{dt}\, dT. \tag{33}$$

Using (22) in (33) gives

$$A = \tfrac{1}{2} qL\beta \int_{t_1}^{t_2} dn_t ,$$

which upon integration yields

$$A = \tfrac{1}{2} qL\beta n_{t0} . \tag{34}$$

Hence A varies *directly* with the heating rate and the *initial electron filling of the trap.*

B. Several Discrete Trapping Levels

If several discrete electron-emitting trapping levels belonging to the same species[7] exist in the energy gap, the total current at any temperature is given by the sum of the thermally stimulated currents from each trap at that temperature. Figure 5(a) shows five distinct TSC curves from five discrete trapping levels, each having the *same* trap density N_t. Since we are concerned with electron-emitting levels, the initial filling of these traps is determined by [see Eq. (15)]

$$\bar{n}_s/(\bar{n}_s + \bar{p}_s + e_n). \tag{35}$$

Since the five trapping levels are members of one and the same species, they have a common quasi-Fermi level for trapped electrons E_{Ft}^n. From (35) the occupancy above E_{Ft}^n (see Sec. IIA and Fig. 3) is very small. This is manifested by the reduced size of the first peak, which is positioned above E_{Ft}^n in energy. Below this level the occupancy is essentially constant and equal to $\bar{n}_s/(\bar{n}_s + \bar{p}_s)$. For this case, the TSC peaks decrease slowly in height the further from the conduction-band edge are the corresponding trap levels. However, the areas under the TSC curves are identical, which simply means that the same amount of charge is released from each trap.

Figure 5 (b) illustrates the case when the five trapping levels are positioned sufficiently close in energy such that each of the corresponding five TSC curves overlaps with the TSC curves of adjacent levels. The TSC curve is much broader than that of an individual TSC curve corresponding to any of the levels involved. The current shows a very sharp rise and decay, and between these extremes it undulates, manifesting several peaks about a large average value. These peaks, of course, relate to the energies of, and provide a means of enumerating, the number of the trapping levels involved. However, the highest and lowest levels in energy of the group do not give rise to separate peaks but only to kinks in the rising and falling portions of the curve.

Figure 5(c) shows the effect produced when the five levels are positioned such that four of the traps are fairly close together in energy. Without knowing otherwise, such a peak can easily be misinterpreted as the TSC response of a discrete level with a large trap density. However, measurements of the temperature of the peak maximum and its half-width would show that this is not the case (see Sec. VI).

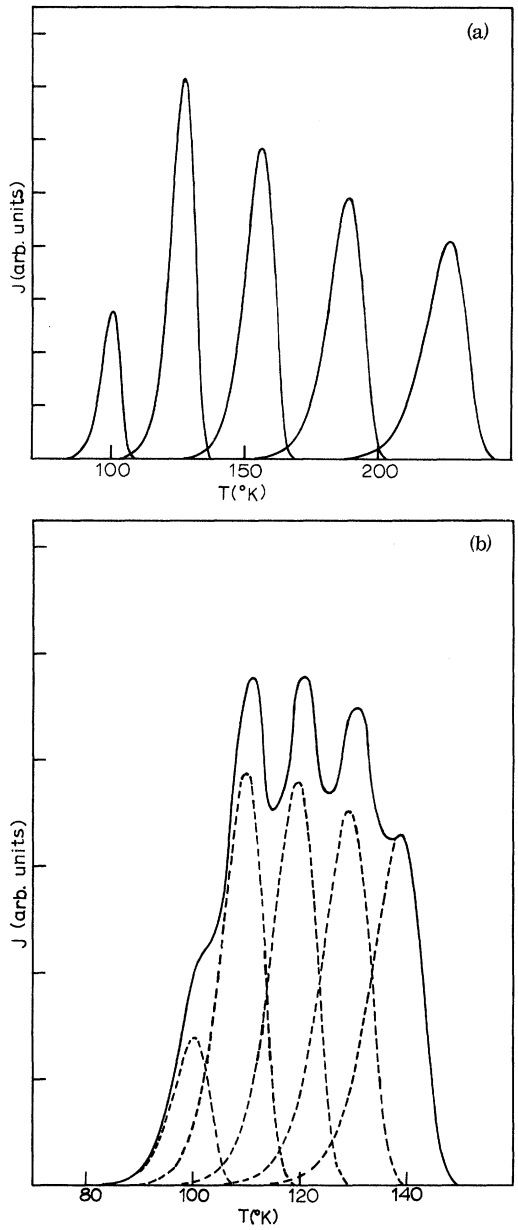

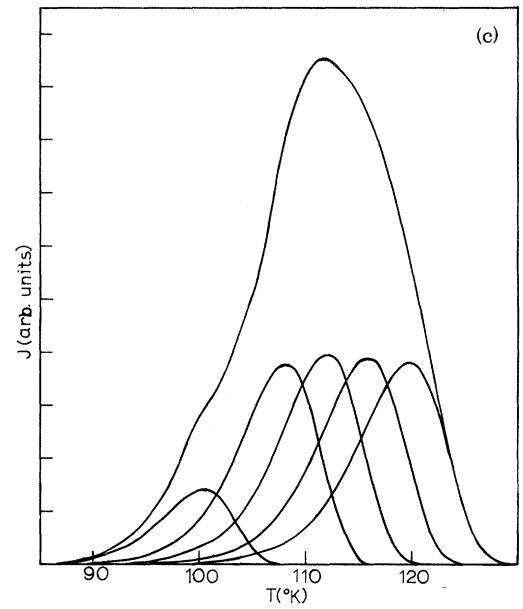

FIG. 5. J-T characteristic for a TSC curve produced by five discrete trapping levels positioned at different energies, illustrating the case of the five levels (a) widely separated in energy; (b) overlapping to produce an undulating response; and (c) overlapping to produce a TSC curve manifesting a single peak.

V. THERMALLY STIMULATED CURRENTS: ANALYTICAL INTERPRETATION

A. E_t vs T_m

One of the difficulties encountered in the understanding of the TSC phenomena and the interpretation of its experimental data lies in the intractable nature of the transcendental relationships which describe the process. The relation (30), which gives the energy of a trapping level in terms of the temperature at which the TSC maximum occurs, has been examined by several authors in an effort to produce a more usable result. It will be noted that (30) may be written

$$e^{\Delta E/kT_m} = v\sigma_n N_c k T_m^2/\beta\Delta E \ . \tag{36}$$

Generally speaking, $v\sigma_n N_c k/\beta\Delta E$ is of the order 10^7, which means that the exponent of the left-hand side of (36) is greater than about 20 for all practical temperatures ($T > 10\ ^\circ$K). If T_m were the only variable in (36), a small change in its magnitude would result in a *large* change in the left-hand side of (36) (because the exponent is a large number) but only a *small* change in the right-hand side. We thus conclude that ΔE must increase almost *linearly* with increasing T_m in order for (36) to be satisfied. This is shown to be the case in Fig. 6, where E is plotted as a function of T_m for various values of s/β, ($s = v\sigma_n N_c$). It is seen that the relationship between ΔE and T_m is approximated very well by a family of straight lines

$$\Delta E = C\,T_m - D,$$

where the slope C is a constant which depends upon s and β and the intercept D which is given by

$$D \simeq 0.0155$$

for all members of the family. The value of C is obtained by constructing a plot (see Fig. 7) of $[(\Delta E + D)/T_m]$ vs $\log_{10}(s/\beta)$ from the data given in Fig. 6. This procedure also yields a straight-line relationship

$$(\Delta E + D)/T_m = B\log_{10}(s/\beta) + Z,$$

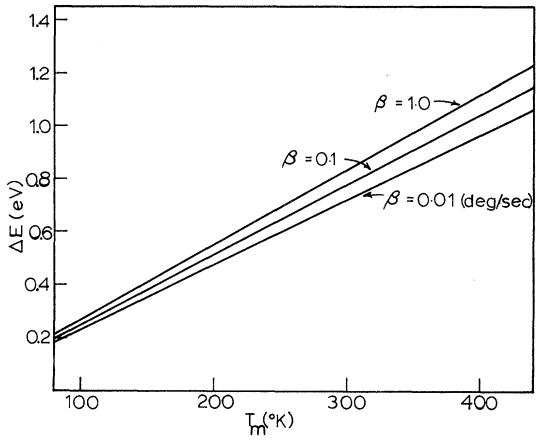

FIG. 6. Family of ΔE vs T_m for three values of heating rate: 0.01, 0.1, and 1.0 deg/sec.

where B $(=1.92\times10^{-4})$ is the slope of the line and $Z(=0.32\times10^{-3})$ is the intercept of the line on the $(\Delta E+D)/T_m$ axis. Thus, within these approximations, ΔE, expressed in electron volts, is given by

$$\Delta E = T_m[1.92\times10^{-4}\log_{10}(s/\beta)+0.32\times10^{-3}] - 0.0155. \quad (37)$$

For practical values of ΔE, s, and β this relationship provides values of ΔE which are accurate to within 2% of the true values obtained from solving the transcendental expression (36).

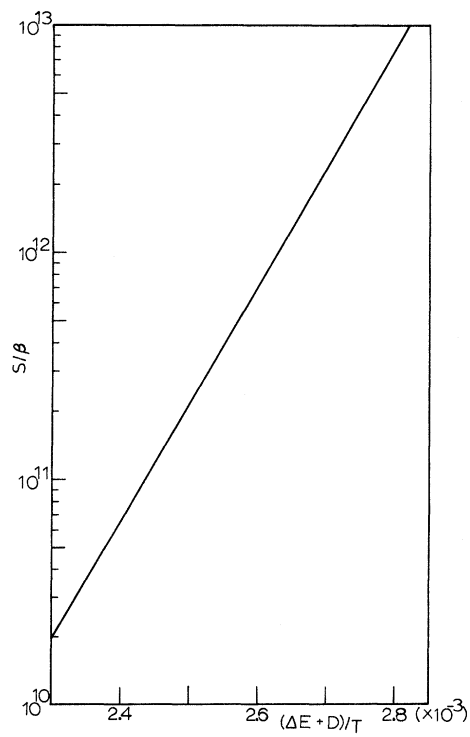

FIG. 7. Plot of $(E_t+D)/T_m$ vs $\log_{10}(s/\beta)$ for several members of the family shown in Fig. 6.

B. Occupancy Functions

From (1), (15), and (24) the non-steady-state statistic of occupancy, at a temperature T, of any trapping level above the intrinsic Fermi level E_i (that is, for $e_n \gg e_p$) is

$$f_n(E,T)=f_0(E)\exp(-\beta^{-1}\int_{T_0}^{T} e_n\,dT). \quad (38)$$

From (1), (15), and (26) the electron occupancy for energy levels below E_i is given by

$$f_n(E,T)=1-[1-f_0(E)]\exp(-\beta^{-1}\int_{T_0}^{T} e_p\,dT) \quad (39)$$

or, in other words, the hole occupancy below E_i is

$$f_p(E,T)=[1-f_0(E)]\exp(-\beta^{-1}\int_{T_0}^{T} e_p\,dT). \quad (40)$$

The exponents

$$\exp(-\beta^{-1}\int_{T_0}^{T} e_n\,dT)\ , \quad (41)$$

$$\exp(-\beta^{-1}\int_{T_0}^{T} e_p\,dT) \quad (42)$$

are the kernels of the high-field TSC solutions [see (23)–(27) and (38)–(40)], but unfortunately they are complicated and intractable. However, they may

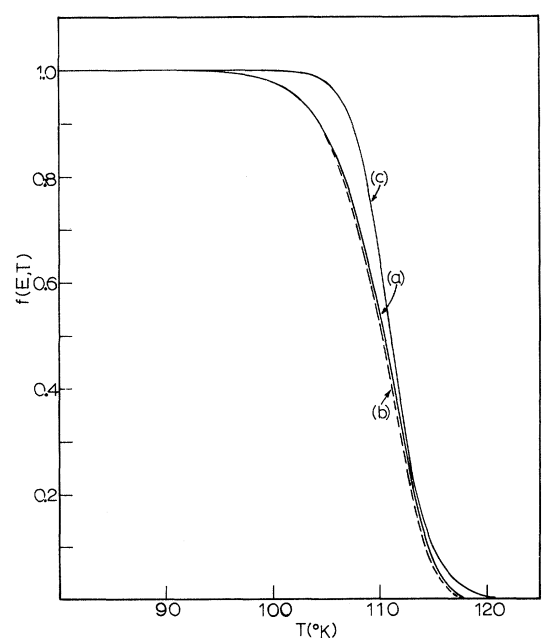

FIG. 8. Plot of the occupancy functions for a TSC curve using (a) transcendental expression (41); (b) approximate expression (43); and (c) modified Fermi-Dirac occupancy function (48).

be expressed in the following approximate analytical forms (see Fig. 8):

$$\exp(-\beta^{-1}\int_{T_0}^{T} e_n\,dT) = e^{-kT^2 e_n/\beta(E_c-E_t)}\,, \tag{43}$$

$$\exp(-\beta^{-1}\int_{T_0}^{T} e_p\,dT) = e^{-kT^2 e_p/\beta(E_t-E_v)}. \tag{44}$$

From (38), (43), and (30) the occupancy of an electron-emitting level at the temperature T_m is

$$f_n(E_t) = f_0(E_t)\,e^{-1}. \tag{45}$$

Similarly, from (40), (44), and (30) the occupancy of a hole-emitting level at the temperature T_m is

$$f_p(E_t) = f_0(E_t)\,e^{-1}. \tag{46}$$

Hence, within the approximation of (43) and (44) any trapping level, regardless of the energy or electron and hole-capture cross sections of the level or of the heating rate, is occupied at the temperature T_m for that level with the fraction e^{-1} of the original occupancy.

C. Quasi-Fermi-Level Concept

The expression (41) behaves very much like a Fermi-Dirac function (see Fig. 8) in that below a certain energy $E_F(T)$ the function takes the value unity, and above $E_F(T)$ it falls rapidly to zero. In fact (39) may be approximated by the *modified* Fermi-Dirac function (see Fig. 8)

$$(1+1.7\,e^{2[E_F(T)-E_t]/kT})^{-1}\,, \tag{47}$$

in which $E_F(T)$ is a parameter, the significance of which is to be discussed a little later. From (38) and (47) the *temperature-* [or time- , see (22)] *dependent* occupancy of an electron-emitting trapping level positioned at an energy E_t is given by

$$f(E) = f_0(E)/(1+1.7\,e^{2[E_F(T)-E_t]/kT}), \tag{48}$$

where the temperature dependence of $E_F(T)$ is given by [see Eq. (37)]

$$E_c - E_F(T) = T[1.92\times10^{-4}\log_{10}(s/\beta) + 0.32\times10^{-3}] - 0.0155. \tag{49}$$

Equation (48) does not provide as accurate an approximation to (41) as (43), but it furnishes some useful physical concepts and a simple analytical expression for the TSC curve, as we shall see shortly.

It will be noted from (48) that the trap occupancy has fallen approximately to e^{-1} of its original occupancy when $E_F(T)$ coincides with the energy (E_t) of the emitting trap level, which from (46) is also the condition for the TSC maximum to occur. This conclusion could also have been reached, by an inspection of (37) and (49), since substituting $T = T_m$ in (49) yields $E_c - E_t = E_c - E_F(T)$, that is, $E_t = E_F(T)$. Thus, it will be apparent that $E_F(T)$ has the characteristics of a non-steady-state quasi-Fermi level because when $E_F(T) > E_t$ the level is substantially occupied and when $E_F(T) < E_t$ the level is essentially empty.

D. Half-Width and Points of Inflection of TSC Peak: Discrete Trap

One of the criteria that may be used for determining whether an experimental TSC curve is due to a single trap or to several traps is the temperature interval $T_2 - T_1$ separating the points of inflexion of the TSC peak (see Fig. 3). Because of the intractable nature of (41), it is not possible to obtain an exact analytical expression for this temperature interval. However, it will be noted (see Fig. 8) that virtually all the change in the Fermi function [occupancy–see (48)] occurs in an energy interval $2kT_m$, centered about the trap energy E_t. This energy interval corresponds to the temperature interval between the points of inflection. In order to relate $2kT_m$ to the temperature range $T_2 - T_1$, we note that ΔE is proportional to T_m [see (37)]. Thus we may write

$$(T_2 - T_1)/2kT_m = T_m/\Delta E,$$

or (50)

$$\Delta T = T_2 - T_1 = 2kT_m^2/\Delta E.$$

This relationship was found to hold extremely well for all TSC curves as shown in Fig. 9. This relationship provides a simple test for the existence of a discrete peak and is a particularly useful one because of its independence of both cross-section and heating rate. On the other hand, if the trap level has already been determined to be discrete, then this relation in conjunction with (37) provides a means of finding the trap cross section for electrons. It will be noted that the temperature interval

$$\delta T = T_b - T_a, \tag{51}$$

corresponding to the temperatures T_b and T_a at which the current attains half its peak value, corresponds reasonably well to the temperature interval $T_2 - T_1$, and this provides a rapid first-order evaluation for TSC curves.

VI. DISCUSSION

A. Identification of Discrete Peak

Existing theories for thermally stimulated currents have dealt almost exclusively with a model which considers only one active discrete trap as an emitting center, together with several "deep traps" and "recombination centers." The latter are intro-

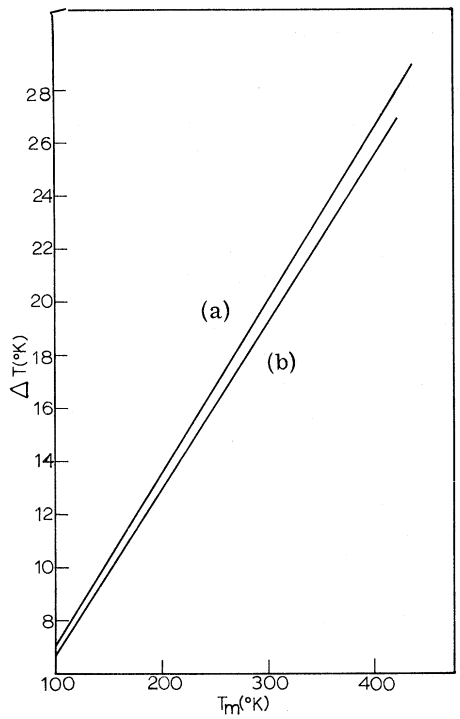

FIG. 9. Plot of ΔT for a TSC curve obtained (a) numerically from the transcendental expression (25) and (b) from approximate formula (50).

duced merely as an artifice to give an air of reality to an otherwise idealistic system. However, in a real crystal the existence of a distribution of trapping centers is more often the case than not.[7]

A group of trapping levels positioned energetically close to each other [see Fig. 5(c)] will often yield a TSC curve manifesting only a single peak and thus can be mistakenly identified as a TSC curve corresponding to a *single* trapping level. However, it is possible to distinguish between the two types of curves because those due to several trapping levels will be much broader than those corresponding to any of the levels existing individually. In fact a good criterion for establishing that a discrete trap level is responsible for a TSC peak is the half-width of the current peak, defined by [see (50) and (51)]

$$\Delta T = 2kT_m^2/\Delta E \ .$$

Using this equation, a value of E_t may be obtained on the assumption that a measured TSC peak corresponds to a discrete trap; also a value of the trap parameter ($s = v\sigma_n N_c$) and hence the cross section σ_n may be determined from (37). Using these parameters, a TSC curve may be constructed according to (29). If the measured TSC peak and the constructed curve (judiciously adjusted so that the two peaks coincide) correlate to a reasonable degree, then one can conclude that a discrete trap level is responsible for the current; otherwise, the curve is due to a number of discrete trap levels or a distribution of trap levels. If the trap level is discrete, and if the initial conditions were exactly reproduced, then the initial filling of the trap n_{t0} may be determined from (31) using two values of I_m corresponding to two values of β.

The analysis of the rising portion of the curve also provides information on the energy depth of the trap and its capture cross section. During the initial rise of the curve, the occupancy of the trap is essentially constant (see Fig. 8), and the current is dominated by, and hence essentially proportional to, e_n for the level. Thus [see (25)] the measurement of the current at two different temperatures in this region of the curve will yield e_n and n_{t0}.

B. Initial Conditions

Unless the same steady-state condition is ensured before each measurement, it is very difficult to correlate successive TSC measurements. The initial boundary conditions are related to the *steady-state* photocurrent that flows in the system just prior to the termination of the excitation. Thus, careful control of the *steady-state photocurrent* can ensure reproducible boundary conditions.

It is interesting to note that, because of the different occupancy functions (7) associated with different species,[7] it is quite possible to have a shallow trap belonging to one species R_1 occupied and a deeper trap belonging to another species R_2 ($> R_1$) essentially empty for the same illumination intensity. As a result, contrary to what is normally expected, the peak of the TSC curve corresponding to the deeper trap appears only for higher-illumination levels than that corresponding to the shallower trap. This again emphasizes the necessity of correlating the illumination intensity with the initial trap occupancy.

C. Temperature Dependence of Parameters

To this point, we have ignored any temperature dependence of the capture cross sections, the thermal velocity, or the effective densities of states (N_c, N_v). Although it is relatively simple to include these dependences in the theory, it will be noted that these parameters always appear together as the product $v\sigma_n N_c$ or $v\sigma_p N_v$ and have the following typical temperature dependences:

$$v \propto T^{1/2} \ , \quad N_c \propto T^{3/2}, \quad \sigma_{n,p} \propto T^{-2}.$$

(The cross-section temperature dependence assumed here applies to a Coulombic type of energy barrier.[9]) Hence, the temperature dependence of their products is negligible. The trap depths ($E_c - E_t$) discussed in the text have been taken as their zero-field values. In actual fact, in the presence of a high field, the energy barrier to electrons and holes

trapped in the bulk will be less than the above due to the Poole-Frenkel lowering effect.[10] If the Poole-Frenkel effect does play a role, and this may be clarified by measuring the TSC at different applied voltages, it may be taken into account through the equation

$$E_t = E_{t0} - \mathcal{E}^{1/2}\,(q^3/\pi K\epsilon_0)^{1/2}\ ,$$

where E_{t0} is the trap energy barrier with no applied field, $\mathcal{E}$ is the applied field strength, ϵ_0 is the permittivity of free space, and K is the high-frequency relative dielectric constant. It will be noted that in the above discussion no mention is made of the mobility of electrons and holes and their temperature dependence. The mobilities are not required in the interpretation of HFTSC (high-field thermally stimulated currents).

D. Generation Statistic

Because of the absence of recombination and retrapping the occupancy function of a particular trap decays from the initial nonequilibrium statistic

$$f(E) = (\bar{n}_s + e_p)/(e_n + \bar{n}_s + \bar{p}_s + e_p)$$

to the high-field trap-occupancy function

$$f(E) = e_p/(e_n + e_p).$$

The latter result may be deduced from the fact that the system is decaying to the state where the rate of emission of holes is just equal to the rate of emission of electrons from all trapping levels. Thus, if N_t is the trap density at an energy E_1 and f is the occupation function then the rate of emission of electrons equals the rate of emission of holes or

$$e_n N_t\ f = e_p N_t\ \ (1-f)\,;$$

hence,

$$f = e_p/(e_n + e_p). \tag{52}$$

Equation (52) is not the thermal-equilibrium statistic tic, i.e., Fermi-Dirac statistic, since from the definitions of e_n and e_p given in Sec. IIA, (52) may be written as follows:

$$f = 1/(1 + e^{2(E_t - E_i)/kT}).$$

This statistic is simply the electron-hole non-equilibrium steady-state-generation statistic. The statistic is symmetric about the intrinsic Fermi energy E_i (where $e_n = e_p$) where it takes the value of $\frac{1}{2}$.

E. Importance of Hole Kinetics

Because of the symmetry of the electron and hole kinetic processes and the similarity between the appropriate equations, remarks similar to those concerning electron emission may be applied to the hole-emitting traps. Because of the indistinguishability between the electron and hole TSC peaks, an observed peak could arise from either an electron- or a hole-emitting trap. A TSC peak due to a group of traps may be produced by a combination of electron- and hole-emitting traps. The capture cross section determined from the measurement may be an electron-capture cross section or a hole-capture cross section, and the energy determined for the level may be with respect to the conduction-band or the valence-band edges.

APPENDIX

Consider the integral

$$\int_{T_0}^{T} e^{-\Delta E/kT}\,dT, \tag{A1}$$

where $\Delta E = E_c - E_t$. This may be integrated by parts in two ways. The first of these is performed directly to yield

$$\int_{T_0}^{T} e^{\Delta E/kT}\,dT = T\,e^{-\Delta E/kT}\Big|_{T_0}^{T} - \int_{T_0}^{T} (\Delta E/kT)\,e^{-\Delta E/kT}\,dT. \tag{A2}$$

The second of these requires a change of variables

$$x = \Delta E/kT,\quad dx = -(\Delta E/kT^2)\,dT, \tag{A3}$$

and the transformation

$$e^{-\Delta E/kT}\,dT = -(\Delta E/k)\,(e^{-x}/x^2)\,dx\ . \tag{A4}$$

Substituting (A3) and (A4) into (A1) and integrating by parts, (A1) may now be expressed as

$$+\frac{\Delta E}{k}\int_{T_0}^{T} \frac{e^{-x}}{x^2}\,dx = -\frac{kT^2}{\Delta E}\,e^{-x}\Big|_{T_0}^{T} + \frac{\Delta E}{k}\int_{T_0}^{T} \frac{2kT}{\Delta E}\,\frac{e^{-x}}{x^2}\,dx\ . \tag{A5}$$

Now when $2kT \ll E$, a good approximation to (A1) from (A5) is

$$\int_{T_0}^{T} e^{-\Delta E/kT}\,dT = \frac{kT^2}{\Delta E}\,e^{-\Delta E/kT} - \frac{kT_0^2}{\Delta E}\,e^{-\Delta E/kT_0}\ . \tag{A6}$$

On the other hand when $kT \gg E$, then a good approximation to (A1) from (A2) is

$$\int_{T_0}^{T} e^{-\Delta E/kT}\,dT = T\,e^{-\Delta E/kT} - T_0\,e^{-\Delta E/kT_0}\ . \tag{A7}$$

On the basis of (A6) and (A7) a general approximation to (A1) for all values of T can be written as

$$\int_{T_0}^{T} e^{-\Delta E/kT}\,dT = [kT^2/(\Delta E + kT)]\,e^{-\Delta E/kT}\ , \tag{A8}$$

where the value at the lower limit T_0 has been dropped in comparison to the value at the upper limit. The accuracy of the approximation is illustrated in Fig. 5 where both (A8) and (A6) are compared with a numerical calculation of the integral (A1).

[1]P. S. Pickard and M. V. Davis, J. Appl. Phys. 41, 2636 (1970).
[2]P. Kelly and P. Braunlich, Phys. Rev. B 1, 1587 (1970).
[3]I. J. Saunders, J. Phys. C 2, 2181 (1969).
[4]R. Chen, J. Appl. Phys. 40, 570 (1969).
[5]K. H. Nicholas and J. Woods, Brit. J. Appl. Phys. 15, 783 (1964).
[6]G. A. Dussel and R. H. Bube, Phys. Rev. 155, 764 (1967).
[7]J. G. Simmons and G. W. Taylor, Phys. Rev. B4, 502 (1971).
[8]J. J. Randell and M. H. F. Wilkens, Proc. Roy. Soc. (London) A184, 366 (1945); A184, 390 (1945).
[9]A. Rose, *Concepts in Photoconductivity and Allied Problems* (Interscience, New York, 1963).
[10]J. G. Simmons, Phys. Rev. 155, 657 (1967).

PHYSICAL REVIEW B VOLUME 5, NUMBER 4 15 FEBRUARY 1972

Multiphoton Transitions in Ionic Crystals

I. M. Catalano, A. Cingolani, and A. Minafra
Istituto di Fisica dell'Universita', Centro Studi e Applicazioni in Tecnologie Avanzate, Bari, Italy
(Received 14 October 1971)

Photoconductivity measurements in uncolored single crystals of NaCl, KCl, and KI are reported. The exciting source is the beam of a Q-switched ruby laser ($\hbar\omega = 1.78$ eV) and its second harmonic ($\hbar\omega = 3.56$ eV). The experimental results show clear evidence of multiphoton absorption processes. The nonlinear cross sections γ_n of two-, three-, four-, and five-photon transitions have been measured and compared with the cross sections predicted by the existing theories.

INTRODUCTION

In the present work we report the results of a study of multiphoton optical transitions in alkali halides.

The absorption process has been detected by means of the associated photocurrent. This method is indeed the only one capable of measuring absorption coefficients as low as 10^{-6} cm^{-1} or less. It may be noted that even with a flux of 10^{26} (photons/cm^2)/sec (which corresponds to about 30 MW/cm^2 of ruby light), the three-photon absorption coefficient is only 10^{-5} cm^{-1} and decreases very rapidly for higher-order transitions.

Other investigations of multiphoton transitions utilizing this technique are reported in the literature[1,2] with experimental results which differ markedly. Our aim was to determine the order of the transition (i.e., the number of photons which participate in the absorption process) and to evaluate the nonlinear cross section γ_n which can be compared with the cross section predicted by existing theories.

EXPERIMENTAL PROCEDURE

The experimental apparatus has been previously described.[3]

A Q-switched ruby laser ($\hbar\omega = 1.78$ eV) with a pulse duration of 20 nsec at half-power and 200-MW peak power was used to induce the photoconductivity. The maximum beam cross section was about 1.5 cm^2. The energy of every pulse was monitored with a photodiode intercepting a small fraction of the beam. The photocurrent pulse is integrated and the resulting voltage pulse is sent to a 556 dual-beam Tektronix oscilloscope with a 1A7A plug-in.

The absolute calibration of the measuring system has been obtained injecting a known amount of charge at the input and recording photographically the voltage output. A linearity test has been performed in the range of interest. The photodiode pulse is also integrated and displayed simultaneously on the other oscilloscope beam, thus giving the energy corresponding to the single photocurrent pulses. The photodiode has been calibrated and tested for linearity by measuring the energy of the laser pulses with a thermocouple calorimeter and the intensity was obtained approximating the photodiode pulse with a square pulse of 20-nsec duration.

To produce a different photon energy a $LiNbO_3$ second-harmonic generator (SHG) has been used in conjuction with the ruby laser. The SHG gives out about 10-MW maximum power at $\hbar\omega = 3.56$ eV and the residual ruby light is filtered out using a cell filled with an aqueous solution of $CuSO_4$.

Undoped monocrystals of NaCl, KCl, and KI, with typical dimension $0.8 \times 0.2 \times 1$ cm^3, were placed